



HAL
open science

Structural and vibrational properties of the van derWaals compound (N₂)₁₁He up to 135 GPa

S. Ninet, G. Weck, P. Loubeyre, F. Datchi

► **To cite this version:**

S. Ninet, G. Weck, P. Loubeyre, F. Datchi. Structural and vibrational properties of the van derWaals compound (N₂)₁₁He up to 135 GPa. *Physical Review B*, 2011, 83 (13), pp.134107. 10.1103/PhysRevB.83.134107 . hal-00595299

HAL Id: hal-00595299

<https://hal.science/hal-00595299>

Submitted on 3 Jul 2023

HAL is a multi-disciplinary open access archive for the deposit and dissemination of scientific research documents, whether they are published or not. The documents may come from teaching and research institutions in France or abroad, or from public or private research centers.

L'archive ouverte pluridisciplinaire **HAL**, est destinée au dépôt et à la diffusion de documents scientifiques de niveau recherche, publiés ou non, émanant des établissements d'enseignement et de recherche français ou étrangers, des laboratoires publics ou privés.

Structural and vibrational properties of the van der Waals compound $(\text{N}_2)_{11}\text{He}$ up to 135 GPaS. Ninet,^{1,2,*} G. Weck,² P. Loubeyre,² and F. Datchi¹¹*Institut de Minéralogie et de Physique des Milieux Condensés, Université Pierre et Marie Curie–Paris 6, CNRS UMR 7590, Paris, France*²*Commissariat à l’Énergie Atomique (CEA)–DPTA, 91680 Bruyères le Châtel, France*

(Received 20 September 2010; revised manuscript received 11 February 2011; published 7 April 2011)

The structural and vibrational properties of the van der Waals compound $(\text{N}_2)_{11}\text{He}$ have been measured up to 175 GPa. The structure, as determined at 14.5 GPa using single-crystal x-ray diffraction, is hexagonal ($P6_3/m$) with seven nonequivalent atoms: 6 N and 1 He. The N_2 molecule centered at (0,0,0) is orientationally disordered. A close relationship with the ε structure of pure solid N_2 is observed. A phase transition to a hexagonal superstructure occurs at 28 GPa, which is attributed to the ordering of these disordered N_2 molecules, driven by quadrupole-quadrupole interaction. A transition to an amorphous state then takes place at 135 GPa. Strong similarities in the structural evolution under pressure of the $(\text{N}_2)_{11}\text{He}$ compound and of $\varepsilon\text{-N}_2$ are discussed.

DOI: [10.1103/PhysRevB.83.134107](https://doi.org/10.1103/PhysRevB.83.134107)

PACS number(s): 64.70.kt, 61.50.Ks, 78.30.-j, 07.35.+k

I. INTRODUCTION

The current interest in the properties of solid nitrogen at ultrahigh pressures has revealed a rich polymorphism. Recent studies have been motivated mainly by the search for nonmolecular, “polymeric” forms of nitrogen in which the triple $\text{N} \equiv \text{N}$ intramolecular bonds are broken, and the N atoms are forming extended covalent single-bonded networks. This has been achieved by compressing N_2 to pressures above 110 GPa, producing either an amorphous solid at ambient temperature¹ or a crystalline cubic phase (phase “cg-N”) at ~ 2000 K.² Associated questions remain unanswered: What are the physical mechanisms driving the amorphization of solid N_2 ? Why is the calculated pressure for the molecular to cg-N transition [50 GPa (Ref. 3)] nearly half the experimental one? The precise knowledge of the crystal structures of solid N_2 in the pressure range 15–150 GPa would be very helpful to progress. Unfortunately, up to now, only the structure of the low-pressure phases of N_2 , i.e., the $\alpha, \beta, \gamma, \delta, \delta^*$ phases, are well understood.^{4–6} Above 15 GPa, the experimental situation is less satisfactory. The proposed $R\bar{3}c$ structure⁷ for $\varepsilon\text{-N}_2$ is incompatible with the measured Raman spectrum above 35 GPa (Refs. 8 and 9) and it is energetically unfavored in *ab initio* calculations.¹⁰ At higher pressures, the structures of the ζ and κ phases are still unknown.¹¹ The determination of the crystal structure of N_2 above 15 GPa has remained an experimental challenge due to the difficulties in producing high-quality samples under these extreme conditions. In particular, the method of growing a single crystal in helium by exploiting the topology of phase separation, as developed for the high-pressure structural studies of solid H_2 (Ref. 12) and of solid O_2 ,¹³ cannot be applied for $\varepsilon\text{-N}_2$ since the He/ N_2 binary phase diagram shows that there is no phase separation between pure solid $\varepsilon\text{-N}_2$ and pure solid helium.¹⁴

By adding a small amount of helium to nitrogen, a stoichiometric compound $(\text{N}_2)_{11}\text{He}$ is formed under pressure.^{14,15} Apart from the hexagonal symmetry and the molecular content (22 N_2 molecules and 2 He atoms) of the unit cell, very little is known about this compound. However, since the amount of He is small and because Raman measurements up to 40 GPa (Ref. 16) have suggested that a close relationship should exist between the structure of the $(\text{N}_2)_{11}\text{He}$ compound and the structure of $\varepsilon\text{-N}_2$, we may anticipate that the properties of this

compound are closely related to those of pure N_2 . Because helium can be used as a soft pressure transmitting medium for this compound, the structure of $(\text{N}_2)_{11}\text{He}$ can be finely studied up to very high pressures. In this paper, we present single-crystal x-ray-diffraction experiments on $(\text{N}_2)_{11}\text{He}$ up to 175 GPa. The structure of $(\text{N}_2)_{11}\text{He}$ is refined at 14.5 GPa. The relationship between the structure of $(\text{N}_2)_{11}\text{He}$ and of N_2 is confirmed and discussed. Also, the succession of phase transitions characterized mimics the one observed in pure N_2 .

II. STRUCTURE OF THE $(\text{N}_2)_{11}\text{He}$ COMPOUND AT 14.5 GPa

The $(\text{N}_2)_{11}\text{He}$ stoichiometric compound was discovered by Vos and collaborators by studying the phase diagram of binary mixtures of N_2 and He.^{14,15} We have checked that for helium concentrations of the initial mixture below $1/12 \approx 8.33$ mol %, this solid compound is in equilibrium with solid nitrogen at $P > 7.9$ GPa [see Fig. 1(b)], while for higher concentrations it is in equilibrium with solid helium at $P > 12$ GPa [see Fig. 1(c)]. The binary phase diagram is represented in Fig. 1(a). $(\text{N}_2)_{11}\text{He}$ samples have been obtained here by compressing in a diamond anvil cell a N_2/He mixture of 3 mol % N_2 . A high-quality single-crystal of $(\text{N}_2)_{11}\text{He}$ [see photograph (c) in Fig. 1], embedded in helium as a hydrostatic pressure-transmitting medium, could be grown at the center of the experimental chamber at 10 GPa. The pressure was measured with the ruby luminescence technique using the quasihydrostatic ruby scale.¹⁸ Angular dispersive x-ray-diffraction experiments with a monochromatic beam were performed at the ID9 and ID27 beamlines of the ESRF. Four different samples were studied up to 30, 60, 97, and 175 GPa, respectively. The Raman spectra have also been measured up to 175 GPa.

The structure of the $(\text{N}_2)_{11}\text{He}$ compound was solved from a data set collected at 14.5 GPa and analyzed with the CrysAlis^{Pro} software (Oxford Diffraction). All the observed diffraction peaks could be related to the same crystal using a hexagonal unit cell. The lattice parameters, $a = 7.936$ Å and $c = 9.360$ Å, agree with those reported by Vos *et al.*¹⁵ A structure solution could be found in the highest possible symmetry space group $P6_3/m$, using direct methods as

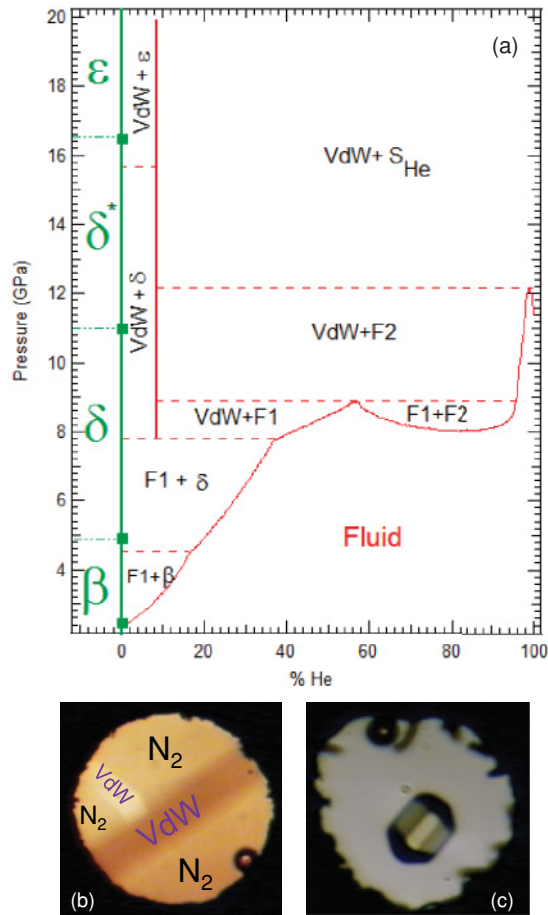


FIG. 1. (Color online) (a) Binary diagram of N_2/He modified from Fig. 1 of Ref. 14. The $(N_2)_{11}He$ compound, denoted VdW, is stable above 7.9 GPa. The sequence of phase transitions in pure solid N_2 is indicated at the left of the figure. (b) Photograph of a sample of 5 mol % He through crossed polarizers at 10 GPa. The photograph shows the phase separation between solid N_2 and the $(N_2)_{11}He$ compound. This coexistence is easily checked by Raman spectroscopy. (c) Photograph of a single crystal of $(N_2)_{11}He$ embedded in helium.

implemented in the SIR97 software.¹⁹ SHELXL97 was used for structure refinement.²⁰ The structure contains seven nonequivalent atoms, 6 N and 1 He. Their final coordinates are given in Table I and a representation of the structure is shown in Fig. 2. The structure solution obtained by SIR97 gave the positions of atoms N_1 to N_5 and He, which then did not change much during the refinement. N_6 was originally placed at the origin but with an anomalously large atomic displacement parameter (ADP). Suppressing this atom from the model and looking at the difference electronic density map, $F_{obs} - F_{calc}$, showed three sharp maxima at $z/c = \pm 0.03$, which suggested three possible orientations for a nitrogen molecule centered at the origin and slightly tilted from the (a,b) plane (see Fig. 3). This was readily modeled by placing the atom N_6 at the position given in Table I with an occupation number of 1/3, since the sixfold symmetry axis generates all the other atoms for the three molecular orientations. When refined freely, the occupation number of N_6 remained close to 1/3 (0.329), indicating that the electron density is well modeled by these

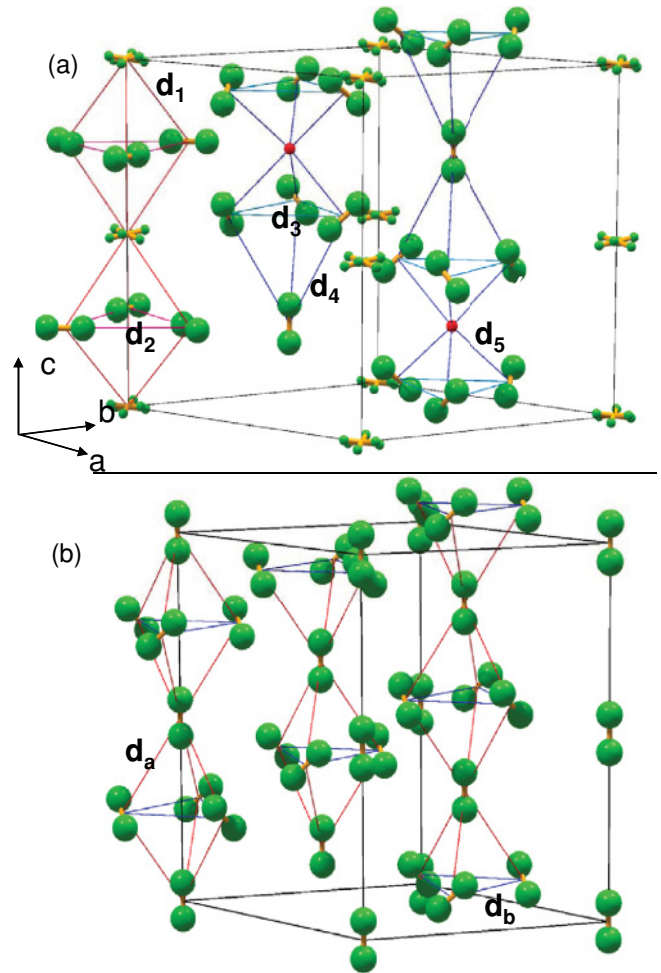


FIG. 2. (Color online) (a) Structure of $(N_2)_{11}He$ (this work). Thin lines are guides to the eyes and show the different trigonal bipyramid. Five different lengths (called d_1 to d_5) characterize these bipyramids. At 14.5 GPa, their values are $d_1 = 3.09 \text{ \AA}$, $d_2 = 3.5 \text{ \AA}$, $d_3 = 3.29 \text{ \AA}$, $d_4 = 3.58 \text{ \AA}$, and $d_5 = 2.51 \text{ \AA}$. (b) Structure of $\epsilon-N_2$ (Ref. 7) in a hexagonal representation [$a = 7.5441 \text{ \AA}$ and $c = 10.5847 \text{ \AA}$ at 17.4 GPa (Ref. 17)]. Thin lines are guides to the eyes and show the trigonal bipyramid. Two different lengths (d_a and d_b) characterize the bipyramid. Their values are $d_a = 3.22 \text{ \AA}$ and $d_b = 3.17 \text{ \AA}$.

three molecular orientations. Moreover, the residual density for the final complete model with isotropic ADP is small (with the highest peak equal to $0.39 e/\text{\AA}^3$ and the lowest peak equal to $-0.33 e/\text{\AA}^3$). We thus conclude that the molecule centered at $(0,0,0)$ is orientationally disordered, with three possible orientations slightly tilted (9.7°) from the hexagonal plane, as shown in Fig. 3(c).

The apparent N-N bond lengths, which were not restrained in the refinement, are 1.021, 1.017, and 1.0136 \AA for the ordered molecules and 1.036 \AA for the disordered ones. The average value is 1.017 \AA for the ordered molecules, i.e., 7.1% shorter than the known value for the gas phase, 1.0976(1) \AA (Ref. 21), and 3.7% shorter than the value determined for the liquid phase by neutron diffraction (1.06 \AA , Ref. 22). However, if we assume that the ordered molecules in $(N_2)_{11}He$ rigidly librate around their center of mass, and that the atomic displacement factors are purely due to molecular libration,

TABLE I. Refined structural parameters of the (N₂)₁₁He $P6_3/m$ structure at 14.5 GPa and 295 K with $a = 7.936$ Å and $c = 9.3600$ Å. A total of 513 reflections, of which 146 unique reflections with $F_{\text{obs}} > 4\sigma$, have been collected. $R_{\text{int}} = 0.1$, $R(F_{\text{obs}} > 4\sigma) = 0.0678$, and $R(\text{all}) = 0.2$, where $R_{\text{int}} = \sum |F_o^2 - \langle F_o^2 \rangle| / \sum F_o^2$, $R = \sum ||F_c| - |F_o|| / \sum |F_o|$.

	x	y	z	Occ.	U_{iso}
N ₁	0.04695	0.6357	-0.10841	1	0.04416
N ₂	-0.33333	0.33333	-0.19571	1/3	0.04215
N ₃	0.15728	0.72018	-0.04097	1	0.04803
N ₄	0.00198	0.30963	-0.25000	1/2	0.04228
N ₅	-0.07229	0.16101	-0.25000	1/2	0.04058
N ₆	0.06931	0.05790	0.00937	1/3	0.04175
He	0.33333	0.66667	-0.25000	1/6	0.03388

then we obtain a thermally corrected covalent bond length of 1.097(4) Å, which is very similar to the gas phase value. Experimental determination of the N-N bond length of pure solid nitrogen is sparse. The structures of the ordered N₂-solid phase [γ -N₂ (Ref. 23) and ϵ -N₂ (Ref. 7)] have been determined with a fixed N-N length around 1.1 Å as in the gas phase. In the disordered δ -N₂, Cromer *et al.*²⁴ reported two different lengths, 0.99 and 1.13 Å at 4.9 GPa and ambient temperature. In the recent work of Stinton *et al.*⁶ on disordered δ^* -N₂, N-N bond lengths are dispersed between 1 and 1.06 Å (1 Å for ex-sphere, 1.05 Å for ex-disk 2, and 1.06 Å for ex-disk 1). These values are in agreement with the N-N bond length determined in this work.

The structure of (N₂)₁₁He is represented in Fig. 2(a). It can be seen as a chainlike arrangement of two types of trigonal bipyramids. In the first chain at the corner of the unit cell, the bipyramid is formed by two identical tetrahedra of N₂ molecules [oriented in the hexagonal (ab) plane] and is characterized by two different lengths: d_1 , between molecules in the basal plane and the molecule at the top of the tetrahedron, and d_2 , between molecules in the basal planes. In the second type, one He atom substitutes one N₂ molecule out of two at the apex of the tetrahedron and the other N₂ molecule points toward the c axis. This leads to an asymmetric bipyramid with three other different distances between N₂ molecules [denoted d_3 , d_4 , and d_5 ; see Fig. 2(a)].

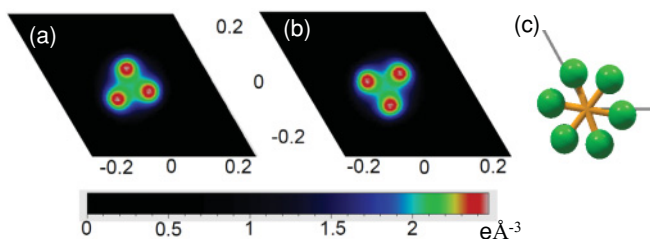


FIG. 3. (Color online) (a) and (b) Difference electron density map ($F_{\text{obs}} - F_{\text{calc}}$) obtained when omitting the atom N₆ in the refinement model. The maps are for two slice cuts along the c axis at $z/c = -0.03$ (left) and $+0.03$ (right), and show half a unit cell in the (a,b) plane centered at (0,0,0). (c) Representation of disordered N₂ molecules centered at (000) (view along the c axis) with three possible orientations.

A factor group analysis shows that there are four Raman-active internal modes corresponding to the four different occupied sites. This agrees with present and previous Raman measurements¹⁶ up to 28 GPa, as shown in Fig. 6. As in pure solid N₂, two separate bands are observed: ν_1 (one peak) and ν_2 (three peaks). The former corresponds to vibrations of molecules located at the top of the bipyramids, while the latter to vibrations of molecules within the basal planes.

Figure 2(b) shows the $R\bar{3}c$ structure of ϵ -N₂,⁷ represented in the hexagonal axes. In this representation, it can be seen as a chainlike arrangement of a regular bipyramid characterized by two different lengths (d_a and d_b). The resemblance with the structure of (N₂)₁₁He is striking [for this reason, we will hereafter refer to the latter structure as ϵ -(N₂)₁₁He]. The two main differences are (i) the substitution of two N₂ molecules by He atoms on sites $6b$ of ϵ -N₂, and (ii) the presence of disordered molecules on the same sites, mainly oriented in the hexagonal plane, in place of ordered molecules aligned along the c axis in ϵ -N₂. This partial orientational disorder in ϵ -(N₂)₁₁He is reminiscent of that present in phases δ -N₂ and δ^* -N₂ at lower pressures.⁶ This could actually indicate that the fully ordered model⁷ for ϵ -N₂ is not correct. We have simulated a model where N₂ molecules at site $6b$ have the same disorder as in ϵ -(N₂)₁₁He. Using the data reported in Ref. 7, we obtain a residual factor $R_{\text{Bragg}} = \sum_{hkl} |I_{hkl}^{\text{obs}} - I_{hkl}^{\text{calc}}| / \sum_{hkl} I_{hkl} = 0.4$, i.e., slightly worse than for the fully ordered model ($R_{\text{Bragg}} = 0.35$). Mills *et al.*⁷ themselves considered a model with spherically disordered molecules and obtained a better R_{Bragg} of 0.25, but this model did not account for one observed reflection. A partial disorder is also suggested by the observation of broad lattice modes in the Raman spectra.²⁵ Moreover, the ordered $R\bar{3}c$ structure only allows for three Raman-active internal modes, whereas five modes are clearly observed above 40 GPa (below the ϵ - ζ transition^{8,9}). We note that the c axis of the compound at 17.4 GPa is 13% smaller than in pure nitrogen ($c[(\text{N}_2)_{11}\text{He}] = 7.858$ Å and $c(\text{N}_2) = 7.54$ Å), whereas the a axis is 4% larger ($a[(\text{N}_2)_{11}\text{He}] = 9.202$ Å and $a(\text{N}_2) = 10.58$ Å). The decrease of the c parameter in (N₂)₁₁He is mainly induced by the presence of helium and not by the planar disorder of the N₂ molecules. That is inferred by looking at the N₂-N₂ distances within the bipyramids. The distance d_1 between the top and basal N₂ molecules of the symmetric bipyramids is similar to the corresponding d_a distance in ϵ -N₂ ($d_1 = 3.05$ Å and $d_a = 3.22$ Å at 17.4 GPa; see Fig. 2). In contrast, the substitution of the N₂ molecule by a He atom shortens this distance considerably ($d_5 = 2.48$ Å at 17.4 GPa), while d_4 (3.53 Å at 17.4 GPa) is slightly larger than d_1 and d_a . We thus conclude that the structure of ϵ -N₂ could present some orientational disorder, which may explain why the $R\bar{3}c$ structure is not found to be the stablest one in *ab initio* calculations.¹⁰

III. STRUCTURAL EVOLUTION AT HIGHER PRESSURE

The diffraction pattern of the (N₂)₁₁He compound has been followed up to 135 GPa. Above 28 GPa, new reflections are observed, as illustrated in Fig. 4. These reflections can be classified in two types: either very weak ones, which can be indexed using a pseudohexagonal supercell ($2a, 2a, c$), as

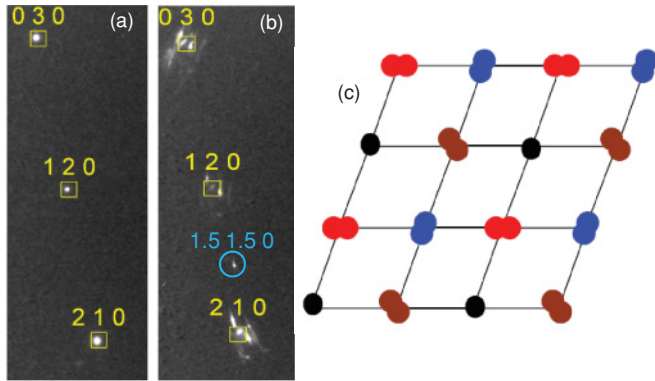


FIG. 4. (Color online) Details of the diffraction image of $(\text{N}_2)_{11}\text{He}$ at 25 GPa (a) and 54 GPa (b). (c) Possible arrangement of the N_2 molecules in the hexagonal (a,b) plane above 28 GPa mapping the pinwheel structure observed in a monolayer of N_2 .²⁶ The previously disordered molecules are frozen. Black circles represent molecules directed along the c axis. Other molecules mostly lie in the hexagonal plane. That order makes a supercell $(2a, 2a, c)$, with a and c being the lattice parameters of the hexagonal cell.

illustrated in Fig. 4 with the $(\frac{3}{2}, \frac{3}{2}, 0)$ reflection; or new ones emerging from the splitting of some initial reflections, which becomes clearer at higher pressures. That splitting increases with the (h,k) indices, whereas the $(00l)$ reflections remain single. We have been unable to find a supercell or a lower symmetry that could account for all the diffraction peaks above 28 GPa. We also observe several splittings in the Raman ν_2 and ν_1 bands above 28 GPa with no frequency discontinuity (see Figs. 5 and 6). These changes are reversible with no hysteresis in pressure. These structural and vibrational observations suggest an ordering of the disordered N_2 molecules at $(0,0,0)$. Indeed, the formation of a hexagonal superlattice is reminiscent of that observed in layers of N_2 or CO molecules on the basal plane of graphite when these molecules orientationally order at low temperatures.^{26,27} Calculations have shown, in this case, that the arrangement and orientation of the molecules are dictated by quadrupolar interactions. It has also been observed that incommensurate arrangements of molecules form in $\text{N}_2/\text{graphite}$ systems for large values of molecular density. A possible ordering of the molecules at the origin in $(\text{N}_2)_{11}\text{He}$, inspired by the pinwheel-type ordering observed in the $\text{N}_2/\text{graphite}$ system, is shown in Fig. 4(c). One out of every four molecules is oriented along the c axis; the other three are planar with three possible orientations, differing by 120° from each other. This arrangement leads to a quasi-hexagonal superlattice $(2a, 2a, c)$. Such a geometry is in agreement with our observation of a pseudo-hexagonal supercell. However, the ordering of quadrupoles on a hexagonal lattice is generally known to lead to frustration, as extensively studied for $\text{N}_2\text{-Ar}$ solid mixtures.²⁸ The topological incompatibility in realizing a minimum possible energy configuration is resolved by an incommensurate modulation of the lattice. The satellite reflections, appearing as peak splittings as seen in Fig. 4, could be the signature of such an incommensurate phase. However, a detailed description of this incommensurate phase could not be resolved with the present x-ray data. Consequently, the proposed incommensurately modulated phase only reflects a reasonable guess to interpret our experimental observations.

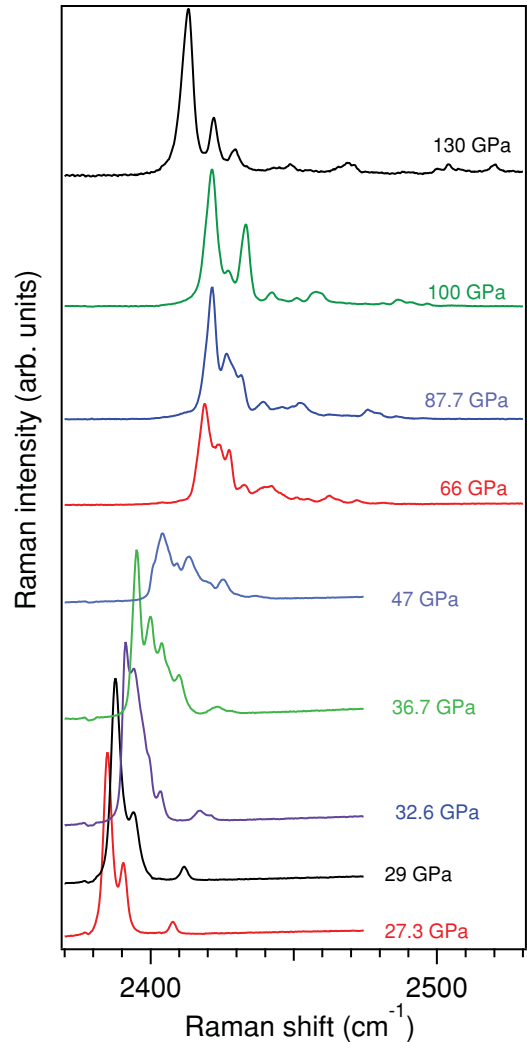


FIG. 5. (Color online) Evolution with pressure of the vibron Raman spectra in $(\text{N}_2)_{11}\text{He}$.

Interestingly, in pure solid N_2 , the splitting of Raman modes above 40 GPa, as shown in Fig. 6, and the change of the x-ray pattern at the $\epsilon\text{-}\zeta$ transition¹¹ are very similar to the present observations in the $(\text{N}_2)_{11}\text{He}$ compound above 28 GPa. It is worth noting that the volume of N_2 at 40 GPa is close to that of $(\text{N}_2)_{11}\text{He}$ at 28 GPa. Since no transition has been reported by x-ray diffraction up to 60 GPa in solid N_2 , Schneider *et al.*⁸ have associated the splitting of Raman modes to slight shifts or changes in orientational ordering coupled with the formation of superlattices. The interpretation in terms of a quadrupolar ordering, as proposed here for $(\text{N}_2)_{11}\text{He}$, would apply if the ϵ phase of solid N_2 had a partial disorder of N_2 molecules, as discussed above, and that cannot be ruled out. The quadrupole-quadrupole interaction seems important enough to control the structural changes in the 50 GPa pressure range in pure solid N_2 and in the $(\text{N}_2)_{11}\text{He}$ compound. This is in contrast to what is obtained in DFT calculations, which do not treat van der Waals interactions correctly.¹⁰

The equation of state (EOS) of $(\text{N}_2)_{11}\text{He}$ is determined up to 135 GPa and it is presented in Fig. 7(b). The volume is calculated using the same x-ray peaks indexed below and above 28 GPa, the satellite reflections being ignored. There is no sign

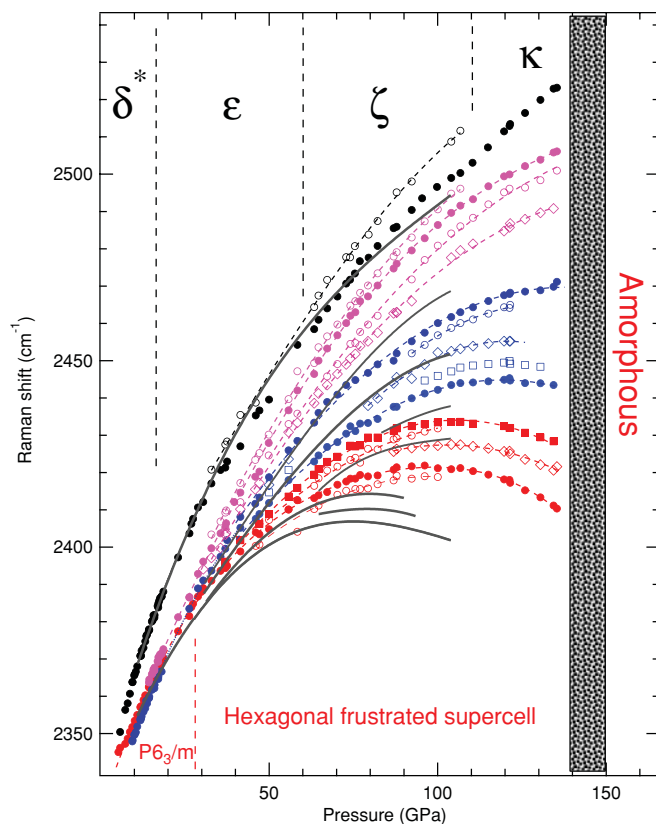


FIG. 6. (Color online) Evolution vs pressure of the N_2 vibron frequency in the $(\text{N}_2)_{11}\text{He}$ compound at 295 K. Symbols represent our experimental data. Dotted lines are a guide to the eyes. For $P < 28$ GPa, four Raman modes are observed. At higher pressure, several splittings occur. Solid and open symbols, respectively, represent the strong and weak intensity modes. The solid lines represent the vibron data in pure solid N_2 .⁹ The sequence of phase transitions in pure solid N_2 and in the $(\text{N}_2)_{11}\text{He}$ compound are indicated at the top and the bottom of the figure, respectively.

of deviatoric stress developing in the sample up to the megabar pressure range, and the agreement between measurements for different samples is excellent. At low pressure ($P < 20$ GPa), our $V(P)$ data are in very good agreement with previous x-ray data of Vos *et al.*,¹⁵ as shown in Fig. 7(b). Up to 28 GPa, the data are well fitted by a Vinet equation.²⁹ Above 28 GPa, the deviation between the extrapolated Vinet EOS and the $V(P)$ data indicates an anomalous change of compressibility, but within the precision of our experiment, no volume jump is detected. This change of compressibility is clearly visible in the plot of the pressure derivative of volume as a function of pressure, as shown in Fig. 7(a). A similar phenomena is observed at the ε - ζ phase transition in solid N_2 , again stressing the similarity between the phase transition in $(\text{N}_2)_{11}\text{He}$ at 28 GPa and that in pure solid N_2 in the 50 GPa pressure range. It should be noted that a change of He concentration in the compound under pressure cannot be the origin of this compressibility change. The solubility of He in solid N_2 exists only for the 1/12 mol % He concentration of the $(\text{N}_2)_{11}\text{He}$ compound, and the Raman spectra, with some modes as a signature of the compound, are reproducible between

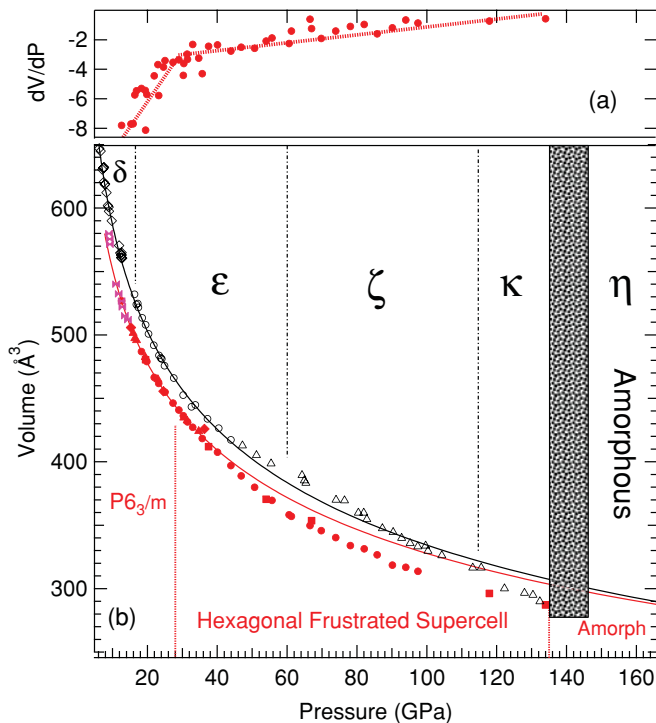


FIG. 7. (Color online) (a) Calculated dV/dP as a function of pressure. Solid lines are guides to the eyes. (b) EOS of $(\text{N}_2)_{11}\text{He}$ at 298 K. Red filled symbols: our data. Pink diamonds: data of Vos *et al.* The solid line is a Vinet fit to the $(\text{N}_2)_{11}\text{He}$ data up to 28 GPa, giving $B_0 = 0.61(3)$ GPa, $B'_0 = 9.1(2)$, and $V_0 = 48.8 \text{ \AA}^3/\text{mol}$. Open symbols represent data on pure N_2 [Δ (Ref. 11), \diamond (Ref. 7), and \circ (Ref. 17)]. The dotted line is the Vinet fit to the ε - N_2 data.¹⁷ The sequence of phase transitions in pure nitrogen and in $(\text{N}_2)_{11}\text{He}$ are indicated at the top and bottom of the figure, respectively.

compression and decompression experiments at least up to 60 GPa.

At 135 GPa, another phase transition is observed. The $(\text{N}_2)_{11}\text{He}$ compound, initially transparent, becomes visually “black,” whereas the helium-transmitting medium remains transparent. This is illustrated in Fig. 8. At the same pressure, the diffraction peaks disappear, and the Raman spectra, measured up to 175 GPa with excitation wavelengths of 488 or 1064 nm, exhibit no modes in any of the frequency regions corresponding to the vibration of single, double, and triple bonded nitrogen. This transition is thus similar to the proposed

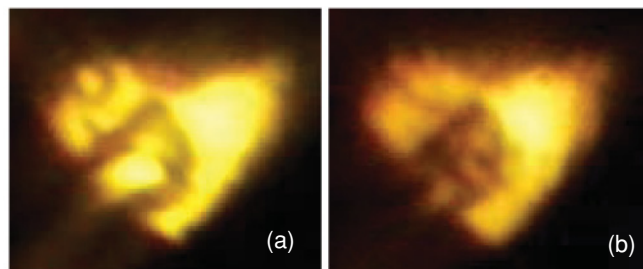


FIG. 8. (Color online) Photographs of the $(\text{N}_2)_{11}\text{He}$ sample surrounded by helium at (a) 125 GPa and (b) 135 GPa. A black compound is visually observed at this phase transition. This is similar to the visually observed amorphization in pure nitrogen.

amorphization of pure N_2 (denoted as η - N_2) observed around 150 GPa.¹

IV. CONCLUSION

In conclusion, by growing a single crystal of the $(N_2)_{11}He$ compound in helium, the structure of this van der Waals compound has been determined. It is hexagonal ($P6_3/m$) with seven nonequivalent atoms: 6 N and 1 He. An orientational disorder of the N_2 molecule centered at (0,0,0) is disclosed. A phase transition is observed at 28 GPa, probably due to a frustrated orientational ordering of the N_2 molecules centered at (0,0,0). A close relationship with the ε - ζ phase transition in solid N_2 is discussed. This should motivate a new look

at the effect of quadrupole-quadrupole interaction to understand the structural changes in solid N_2 in the 50 GPa range. Finally, the $(N_2)_{11}He$ compound is remarkably stable under pressure, at least up to 135 GPa. It would be very interesting now to investigate if these He impurities can help to stabilize new forms of poly-N by extending the present measurements to high temperatures.

ACKNOWLEDGMENTS

We acknowledge the ESRF for provision of beam time under proposals HS3519 and HS3543. We wish to thank M. Mezouar (ID27), M. Merlini, and M. Hanfland (ID09) for their help with x-ray-diffraction experiments.

*sandra.ninet@impmc.upmc.fr

¹E. Gregoryanz, A. F. Goncharov, R. J. Hemley, and H. K. Mao, *Phys. Rev. B* **64**, 052103 (2001).

²M. I. Eremets, R. J. Hemley, H. K. Mao, and E. Gregoryanz, *Nature (London)* **411**, 170 (2001).

³C. Mailhot, L. H. Yang, and A. K. McMahan, *Phys. Rev. B* **46**, 14419 (1992).

⁴*Physics of Cryocrystals*, edited by V. Manzhelli and Y. Freiman (AIP, New York, 1996).

⁵H. Katzke and P. Toledano, *Phys. Rev. B* **78**, 64103 (2008).

⁶G. W. Stinton, I. Loa, L. F. Lundegaard, and M. I. McMahon, *J. Chem. Phys.* **131**, 0104511 (2009).

⁷R. Mills, B. Olinger, and D. Cromer, *J. Chem. Phys.* **84**, 2837 (1985).

⁸H. Schneider, W. Häfner, A. Wokaun, and H. Olijnyk, *J. Chem. Phys.* **96**, 8046 (1992).

⁹H. Olijnyk and A. P. Jephcoat, *Phys. Rev. Lett.* **83**, 332 (1999).

¹⁰C. J. Pickard and R. J. Needs, *Phys. Rev. Lett.* **102**, 125702 (2009).

¹¹E. Gregoryanz, A. F. Goncharov, C. Sanloup, M. Somayazulu, H. K. Mao, and R. J. Hemley, *J. Chem. Phys.* **126**, 184505 (2007).

¹²P. Loubeyre, R. Le Toullec, D. Hausermann, M. Hanfland, R. J. Hemley, H. K. Mao, and L. W. Finger, *Nature (London)* **383**, 702 (1996).

¹³L. Lundegaard, G. Weck, M. McMahon, S. Desgreniers, and P. Loubeyre, *Nature (London)* **443**, 201 (2006).

¹⁴W. L. Vos and J. A. Schouten, *J. Low Temp. Phys.* **19**, 338 (1993).

¹⁵W. L. Vos, L. W. Finger, R. J. Hemley, J. Z. Hu, H. K. Mao, and J. A. Schouten, *Nature (London)* **358**, 46 (1992).

¹⁶H. Olijnyk and A. Jephcoat, *J. Phys. Condens. Matter* **9**, 11219 (1997).

¹⁷H. Olijnyk, *J. Chem. Phys.* **93**, 8968 (1990).

¹⁸H. K. Mao, J. Xu, and P. Bell, *J. Geophys. Res.* **91**, 4673 (1986).

¹⁹A. Altomare, M. Burla, M. Camalli, G. Cascarano, C. Giacovazzo, A. Guagliardi, A. Moliterni, G. Polidori, and R. Spagna, *J. Appl. Cryst.* **32**, 115 (1999).

²⁰G. Sheldrick, *Acta Cryst. A* **64**, 112 (2008).

²¹B. P. Stoicheff, *Can. J. Phys.* **32**, 630 (1954).

²²J. Clarke, J. Dore, and R. Sinclair, *Mol. Phys.* **29**, 581 (1975).

²³R. Mills and A. Schuch, *Phys. Rev. Lett.* **23**, 1154 (1969).

²⁴D. Cromer, R. L. Mills, D. Schiferl, and L. A. Schwalbe, *Acta Crystallogr. Sec. B* **37**, 8 (1981).

²⁵R. Bini, L. Ulivi, J. Kreutz, and H. Jodl, *J. Chem. Phys.* **112**, 8522 (2000).

²⁶K. Morishige, C. Mowforth, and R. Thomas, *Surf. Sci.* **151**, 289 (1985).

²⁷S. E. Roosevelt and L. W. Bruch, *Phys. Rev. B* **41**, 12236 (1990).

²⁸J. A. Hamida, N. S. Sullivan, and M. D. Evans, *Phys. Rev. Lett.* **73**, 2720 (1994).

²⁹P. Vinet, J. Ferrante, J. R. Smith, and J. H. Rose, *J. Phys. C* **19**, L467 (1986).